Exciting the long-lived Higgs mode in superfluid Fermi gases with particle removal

Guitao Lyu,[1,*] Kui-Tian Xi,[1,2,3,†] Sukjin Yoon,[4,5,6] Qijin Chen,[7,8,9,‡] and Gentaro Watanabe[1,10,§]

[1]*School of Physics and Zhejiang Institute of Modern Physics, Zhejiang University, Hangzhou, Zhejiang 310027, China*
[2]*College of Physics, Nanjing University of Aeronautics and Astronautics, Nanjing 211106, China*
[3]*Key Laboratory of Aerospace Information Materials and Physics (NUAA), MIIT, Nanjing 211106, China*
[4]*Center for Theoretical Physics of Complex Systems, Institute for Basic Science, Daejeon 34051, Korea*
[5]*Asia Pacific Center for Theoretical Physics, Pohang, Gyeongsangbuk-do 37637, Korea*
[6]*Quantum Universe Center, Korea Institute for Advanced Study, Seoul 02455, Korea*
[7]*Hefei National Research Center for Physical Sciences at the Microscale and School of Physical Sciences, University of Science and Technology of China, Hefei, Anhui 230026, China*
[8]*Shanghai Research Center for Quantum Science and CAS Center for Excellence in Quantum Information and Quantum Physics, University of Science and Technology of China, Shanghai 201315, China*
[9]*Hefei National Laboratory, University of Science and Technology of China, Hefei 230088, China*
[10]*Zhejiang Province Key Laboratory of Quantum Technology and Device, Zhejiang University, Hangzhou, Zhejiang 310027, China*

(Received 18 October 2022; accepted 10 February 2023; published 23 February 2023)

Experimental evidence of the Higgs mode in strongly interacting superfluid Fermi gases had not been observed until recently [Behrle *et al.*, Nat. Phys. **14**, 781 (2018).]. Due to the coupling with other collective modes and quasiparticle excitations, generating stable Higgs-mode oscillations is challenging. We study how to excite long-lived Higgs-mode oscillations in a homogeneous superfluid Fermi gas in the BCS-BEC crossover. We find that the Higgs mode can be excited by time-periodically modulating the scattering length at an appropriate amplitude and frequency. However, even for a modulation frequency below twice the pairing-gap energy, quasiparticles are still excited through the generation of higher harmonics due to nonlinearity in the superfluid. More importantly, we find that persistent Higgs-mode oscillations with almost constant amplitude can be produced by removing particles at an appropriate momentum, and the oscillation amplitude can be controlled by the number of removed particles. Finally, we propose two ways to experimentally realize particle removal.

DOI: 10.1103/PhysRevA.107.023321

I. INTRODUCTION

The Higgs mode is an amplitude oscillation of the Higgs field which plays an important role in mass generation for elementary particles via spontaneous symmetry breaking [1–3]. As an analogy, the Higgs mode in condensed-matter systems refers to an amplitude oscillation of the order parameter related to the spontaneous breaking of a continuous symmetry [4–6]. While the excitation and detection of the Higgs mode in high-energy experiments require extremely large-scale facilities such as the Large Hadron Collider at CERN, they are feasible with tabletop experiments for condensed-matter systems [7–17]. Therefore, the latter is an important test bed for studying the Higgs mode and has been drawing attention, especially after the detection of the Higgs boson in high-energy experiments in 2012 [18,19].

The first work on the Higgs mode in condensed matter was done by Volkov and Kogan around a half century ago [20], although it was not called the Higgs mode at that time. They found that the frequency of the Higgs mode in the superconductor is $\simeq 2\Delta_0/\hbar$ (Δ_0 is the pairing gap in equilibrium) and the amplitude decays with time t in a power law of $t^{-1/2}$. However, in the context of the BCS-BEC crossover in superfluid Fermi gases, it was predicted that the amplitude decay follows a different power law of $t^{-3/2}$ in the Bose-Einstein condensation (BEC) regime [21], unlike the $t^{-1/2}$ behavior in the BCS regime. The earliest evidence for the existence of the Higgs mode was found in superconductors [7], where unexpected peaks in Raman scattering were revealed to be the Higgs mode [22,23]. Since the realization of degenerate atomic Fermi gases [24], there have been many theoretical studies on the Higgs mode in superfluid Fermi gases with various types of external drives, such as a sudden quench [21,25–35], ramping [36–38], time-periodic modulation of the interaction strength [36,37,39–41], and so on [42,43]. The visibility of the Higgs mode in fermionic superfluids has also been studied [44–46]. Regarding the small oscillations around the equilibrium state after quench, a decay is inevitable in homogeneous three-dimensional systems in the BCS-BEC crossover since the Higgs mode is coupled with the Goldstone mode due to the absence of particle-hole symmetry [47]. On the other hand, when the initial perturbation is sufficiently large or for some particular nonequilibrium initial states, persistent Higgs-mode oscillations have been predicted to be possible [26,28–30]. Generating stable Higgs-mode oscillations is important for future practical applications. For example, persistent Higgs-mode oscillations enable us to probe the information about the

*guitao@zju.edu.cn
†xiphys@nuaa.edu.cn
‡qjc@ustc.edu.cn
§gentaro@zju.edu.cn

material phase, such as the interband couplings in multiband superconductors (see, e.g., Refs. [48–50]) and the superconductivity in photoinduced states (see, e.g., Refs. [51–54]). A long-lived Higgs mode is also possible in trapped two-dimensional Fermi gases, where the trapping confinement can stabilize the Higgs mode by making its decay channels discrete [55]. However, experimental evidence for the Higgs mode in atomic superfluid Fermi gases was observed only recently [17] because generating stable Higgs-mode oscillations against decay has been challenging.

In the present paper, we propose a scheme for generating long-lived Higgs-mode oscillations in a homogeneous superfluid Fermi gas in the BCS-BEC crossover. We approach this problem by numerical simulations of the time-dependent Bogoliubov–de Gennes (BdG) equations. First, we consider time-periodic modulations of the scattering length in the BCS-BEC crossover. A basic idea behind this scheme is to sustain the Higgs-mode oscillations against decay by a continuous drive. Although this scheme can generate Higgs-mode oscillations, other unwanted excitations are also created due to the nonlinearity of the BdG equations. As an alternative scheme to excite the Higgs mode, we propose an unconventional type of quench by removing particles around a certain momentum. This scheme can generate stable and persistent Higgs-mode oscillations whose lifetime and amplitude are much larger than those observed in a recent experiment [17]. By tuning the momentum of the removed particles at the peak of the pair wave function F_k, the long-lived Higgs mode can be excited. Furthermore, the amplitude of the oscillations can be controlled by the number of removed particles. The long lifetime and large amplitude are strong advantages for future experimental detections and investigations. Particularly, the amplitude of the oscillations excited by this scheme remains almost constant for a long time instead of experiencing prompt power-law decay.

This paper is organized as follows. In Sec. II, we present the formulation of our simulations. In Sec. III, we discuss the scheme using the time-periodic modulation of the scattering length and its resulting higher-harmonic excitations. The scheme of removing particles will be discussed in Sec. IV. In Sec. V, we summarize our work and discuss how to experimentally realize the particle removal.

II. FORMULATION

We consider a homogeneous superfluid Fermi gas at zero temperature in the BCS-BEC crossover. Our system consists of attractively interacting unpolarized (pseudo)spin-1/2 fermionic atoms. The time evolution of the pairing gap $\Delta(t)$ is studied by numerically solving the time-dependent Bogoliubov–de Gennes (TD-BdG) equations [56–58]:

$$i\hbar\frac{d}{dt}\begin{bmatrix}u_{\boldsymbol{k}}(t)\\ v_{\boldsymbol{k}}(t)\end{bmatrix}=\begin{bmatrix}H' & \Delta(t)\\ \Delta^*(t) & -H'\end{bmatrix}\begin{bmatrix}u_{\boldsymbol{k}}(t)\\ v_{\boldsymbol{k}}(t)\end{bmatrix}, \tag{1}$$

where $H'\equiv\hbar^2k^2/(2m)-\mu=\epsilon_k-\mu$ is the single-particle Hamiltonian with wave number $k=|\boldsymbol{k}|$ and $\epsilon_k\equiv\hbar^2k^2/2m$, m is the mass of an atom, and μ is the chemical potential of the reference equilibrium state introduced for convenience to remove the fast rotation of the overall phase. (In our simulations, the initial equilibrium state is taken as the reference state.) The time-dependent quasiparticle amplitudes $u_{\boldsymbol{k}}(t)$ and $v_{\boldsymbol{k}}(t)$ satisfy the normalization condition: $|u_{\boldsymbol{k}}(t)|^2+|v_{\boldsymbol{k}}(t)|^2=1$. The pairing gap reads

$$\Delta(t)=-\frac{g}{V}\sum_{\boldsymbol{k}}u_{\boldsymbol{k}}(t)\,v_{\boldsymbol{k}}^*(t)=-\frac{g}{V}\sum_{\boldsymbol{k}}F_{\boldsymbol{k}}(t), \tag{2}$$

where g is the coupling constant of the contact interaction and V is the volume of the system. Here,

$$F_{\boldsymbol{k}}(t)\equiv u_{\boldsymbol{k}}(t)\,v_{\boldsymbol{k}}^*(t) \tag{3}$$

is the pair wave function. The number density n of atoms is

$$n=\frac{2}{V}\sum_{\boldsymbol{k}}|v_{\boldsymbol{k}}(t)|^2=\frac{2}{V}\sum_{\boldsymbol{k}}n_{\boldsymbol{k}}(t), \tag{4}$$

with

$$n_{\boldsymbol{k}}(t)\equiv|v_{\boldsymbol{k}}(t)|^2 \tag{5}$$

being the momentum distribution of atoms (either spin up or spin down). The energy density $\mathcal{E}$ is given by

$$\mathcal{E}=\frac{2}{V}\sum_{\boldsymbol{k}}\epsilon_k|v_{\boldsymbol{k}}(t)|^2+\frac{1}{g}|\Delta(t)|^2. \tag{6}$$

All the summations here are restricted to the energy range $0\leqslant\epsilon_k\leqslant E_c$, where $E_c\equiv\hbar^2k_c^2/2m$ is the cutoff energy (k_c is the cutoff wave number), and the coupling constant g is renormalized as [59–61]

$$\frac{1}{g}=\frac{m}{4\pi\hbar^2a}-\frac{1}{V}\sum_{k\leqslant k_c}\frac{1}{2\epsilon_k}=\frac{m}{4\pi\hbar^2a}-\frac{mk_c}{2\pi^2\hbar^2}, \tag{7}$$

where a is the s-wave scattering length.

In our numerics, we first solve self-consistently the gap equation (2) and the number equation (4) for the equilibrium solution for $\{u_{\boldsymbol{k}}\}$ and $\{v_{\boldsymbol{k}}\}$ by tuning the chemical potential in an iterative way. Then we treat the equilibrium solution as the initial state and solve the TD-BdG equations (1) in momentum space using the fifth-order Adams-Bashforth backward predictor-corrector method. In each step of the time integration, the corrector step is iterated until the absolute error of all $u_{\boldsymbol{k}}$ and $v_{\boldsymbol{k}}$ is less than 10^{-6}. The step size δk of the momentum grid is taken to be $\delta k=0.001k_F$. The time step δt is typically taken to be $\delta t=0.0005\hbar/E_F$ but is allowed to be adjusted to reach convergence.

III. HIGHER-HARMONIC EXCITATIONS FROM TIME-PERIODIC MODULATION

First, we consider time-periodic modulation of the coupling constant g, which can be experimentally achieved by modulating the magnetic field near a Feshbach resonance [62–64] (see also Ref. [65] and references therein). The coupling constant g is periodically modulated around the initial value g_0 as

$$g(t)=g_0(1+A\sin\omega t), \tag{8}$$

where A and ω are the modulation amplitude and frequency, respectively.

In the simulation, we initially prepare the equilibrium state at zero temperature for a given value of the interaction strength $1/k_Fa$, where $k_F=(3\pi^2n)^{1/3}$ is the Fermi wave

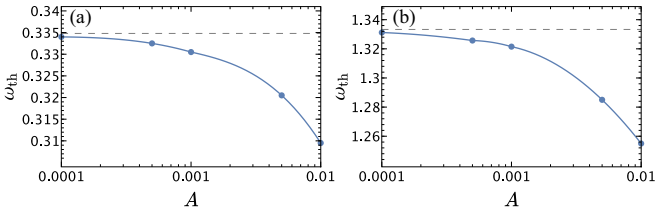

FIG. 1. Threshold frequency $\omega_{\rm th}$ (in units of $E_F/\hbar$) as a function of the modulation amplitude A for (a) $1/k_F a = -1$ and (b) 0. The horizontal dashed lines show $2|\Delta_0|/\hbar$, where Δ_0 is the pairing gap in the equilibrium state for the same value of $1/k_F a$.

number of a uniform ideal Fermi gas with the same density n. From Eq. (7), this given value of $1/k_F a$ and the corresponding initial coupling constant g_0 are related as

$$\frac{1}{k_F a} = \frac{4\pi\hbar^2}{m}\frac{1}{k_F g_0} + \frac{2}{\pi}\sqrt{\frac{E_c}{E_F}}, \tag{9}$$

with $E_F \equiv \hbar^2 k_F^2/2m$. Starting from this initial equilibrium state, we solve the TD-BdG equations (1) under the time-periodic modulation of the coupling constant given by Eq. (8).

By diagonalizing the matrix on the right-hand side of Eq. (1) for the stationary state, one can readily obtain the quasiparticle spectrum $\pm E_k$ in the equilibrium state given by

$$E_k = \sqrt{(\epsilon_k - \mu)^2 + |\Delta_0|^2}. \tag{10}$$

Here, Δ_0 is the equilibrium value of the pairing gap, which can be determined self-consistently from Eqs. (2) and (4).

A. Threshold frequency in the small-amplitude limit

Let us first focus on the small modulation amplitude $A \ll 1$. When the modulation frequency ω is sufficiently small such that $\hbar\omega \ll |\Delta|$, the system follows the modulation adiabatically, and the energy density $\mathcal{E}$ just shows a small amplitude oscillation due to the time-periodic change in the coupling constant $g(t)$. In this case, there are no excitations created. However, above a threshold frequency $\omega_{\rm th}$, i.e., $\omega \gtrsim \omega_{\rm th}$, the energy density $\mathcal{E}$ shows a gradual increase in time in addition to the small amplitude oscillation. Figure 1 shows $\omega_{\rm th}$ as a function of A for $1/k_F a = -1$ [Fig. 1(a)] and 0 [Fig. 1(b)]. Here, we see that, for nonzero modulation amplitude A, $\omega_{\rm th}$ is slightly smaller than $2|\Delta_0|/\hbar$ (the dashed lines), corresponding to the threshold energy of the pair-breaking excitation for the equilibrium system (note that $\mu > 0$ for both $1/k_F a = -1$ and 0). This is due to the reduction in the minimum value of $|\Delta(t)|$ from Δ_0 directly caused by the reduction in the coupling constant $g(t)$ from g_0 to $g_0(1-A)$ for nonzero A. Note that $\omega_{\rm th}$ approaches $2|\Delta_0|/\hbar$ in the limit of $A \to 0$, as expected. On the other hand, in the sufficiently deep BEC regime with $\mu < 0$ (e.g., at $1/k_F a = 1$), the threshold frequency $\omega_{\rm th}$ is $2\sqrt{\mu^2 + |\Delta_0|^2}/\hbar$ in the limit of $A \to 0$, as can be seen from Eq. (10).

B. Resonance peaks and higher-harmonic generation

Now, we employ the time-periodic modulation of g to excite the Higgs mode. By tuning the modulation frequency ω around $2|\Delta_0|/\hbar$ just above $\omega_{\rm th}$ [20], we can resonantly

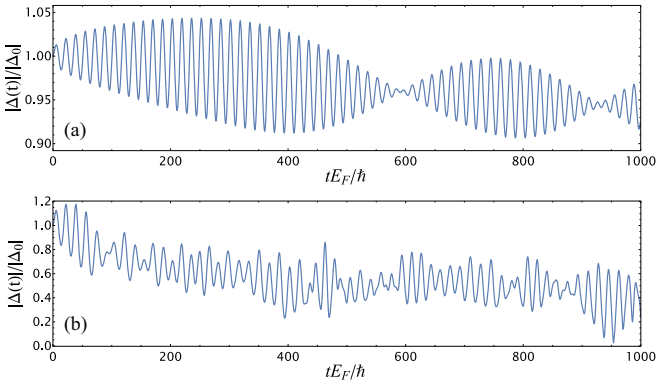

FIG. 2. Oscillation of the pairing gap $|\Delta(t)|$ driven by the time-periodic modulation of the coupling constant $g(t)$ given by Eq. (8). Here, we take the modulation frequency $\omega = 2|\Delta_0|/\hbar$ and $1/k_F a = -1$. In (a) and (b), we take the modulation amplitude $A = 0.001$ and 0.01, respectively.

excite the oscillation of the magnitude of the pairing gap $\Delta(t)$. Figure 2(a) shows an example of the resulting pairing dynamics induced by the time-periodic modulation of g with $\omega = 2|\Delta_0|/\hbar$ and very small amplitude $A = 0.001$. Here, we can see that, in addition to the oscillation with a constant frequency at $\simeq 2|\Delta_0|/\hbar$, which corresponds to the Higgs mode, there is a clear signature of beating, and the amplitude of its envelope decreases in time. Such a diminishing beat is evidence that the time-periodic modulation of g excites not only the Higgs mode but also other unwanted collective modes and quasiparticles.

Furthermore, in addition to the collective modes, various single-particle excitations are also created by the modulation of g at a larger amplitude A and/or after a sufficiently long time. One prominent phenomenon is the higher-harmonic generation by the parametric up-conversion discussed below (see also Ref. [40]). Due to these excitations, the oscillation of $|\Delta(t)|$ becomes irregular, as shown in Fig. 2(b) for $A = 0.01$. To see the mechanism of higher-harmonic generation, we first write the pairing gap $\Delta(t)$ as $\Delta(t) = g(t)\,\tilde{\Delta}(t)$, with $\tilde{\Delta}(t) \equiv -V^{-1}\sum_{\boldsymbol{k}} u_{\boldsymbol{k}}(t)\, v^*_{\boldsymbol{k}}(t)$. Suppose that $\tilde{\Delta}(t)$ initially synchronizes with the modulation of the coupling constant $g(t)$, so that it oscillates at the modulation frequency ω. Since $g(t)$ also oscillates at ω, their product $g(t)\,\tilde{\Delta}(t)$ has the second-harmonic component with doubled frequency 2ω. Once $\tilde{\Delta}(t)$ has the component of 2ω, $g(t)\,\tilde{\Delta}(t)$ will have the third-harmonic component with 3ω. Likewise, further higher-harmonic excitations are also generated. This phenomenon is analogous to the parametric up-conversion in nonlinear optics (see, e.g., [66]).

Due to the higher-harmonic generation, we can observe growing peaks (and dips) in the momentum distribution n_k and the pair wave function F_k during the time evolution. Furthermore, even if the modulation frequency is smaller than the threshold frequency $\omega_{\rm th} \lesssim 2|\Delta_0|/\hbar$ for $\mu \geqslant 0$ or $\omega_{\rm th} \lesssim 2\sqrt{\mu^2 + |\Delta_0|^2}/\hbar$ for $\mu < 0$, resonance peaks and dips can appear by the higher harmonics. For example, Fig. 4 shows snapshots of n_k and F_k at $t = 2000/(E_F/\hbar)$ from the BCS (top panels) to BEC (bottom panels) regime. The positions of these peaks (and dips) are consistent with the resonance condition

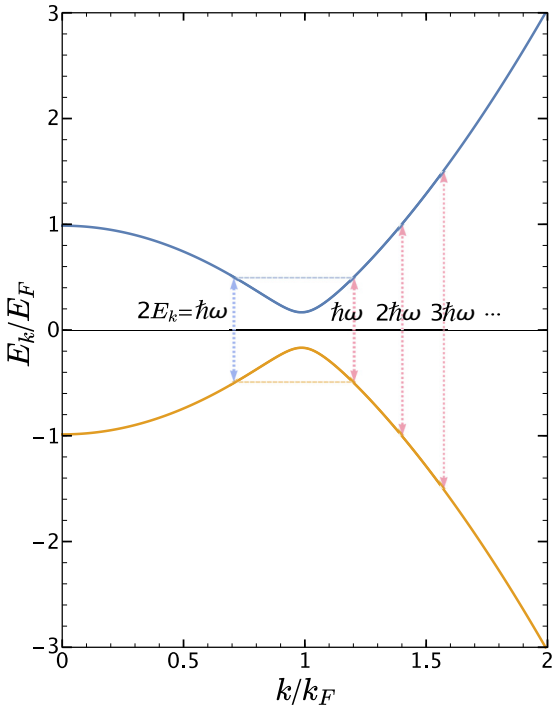

FIG. 3. Quasiparticle spectra $\pm E_k$ and positions of the resonance peaks for the fundamental and higher harmonics. This plot is shown for $1/k_F a = -1$ and $\omega = 1E_F/\hbar$ as an example.

(see Fig. 3):

$$2E_k = l\hbar\omega \quad (l = 1, 2, 3, \dots), \tag{11}$$

with the quasiparticle spectrum E_k given by Eq. (10).

Note that, when $\mu > 0$ so that E_k is not monotonically increasing with k, modulation with ω satisfying

$$2|\Delta_0| < l\hbar\omega < 2\sqrt{\mu^2 + |\Delta_0|^2} \tag{12}$$

yields two resonance peaks (and dips) with the same value of l. See, e.g., the two vertical arrows for $2E_k = \hbar\omega$ in Fig. 3. As an example, Figs. 4(a) and 4(b) show the case of $1/k_F a = -1$ (BCS side, $\mu > 0$) with $\omega = 1E_F/\hbar$, which satisfies Eq. (12) for $l = 1$ ($\mu \approx 0.95E_F$ and $\Delta_0 \approx 0.21E_F$ at $1/k_F a = -1$ in the mean-field theory). There are two peaks (and dips) in n_k and F_k at $k/k_F \approx 0.7$ and 1.2, and the positions of these peaks and dips are consistent with the resonance condition (11) (marked by the vertical dotted line) for $l = 1$. There is another peak and dip at $k/k_F \approx 1.4$, which corresponds to the resonance condition (11) for $l = 2$. Figures 4(c) and 4(d) show the case at unitarity ($1/k_F a = 0$) with $\omega = 3E_F/\hbar$. Although $\mu > 0$ at unitarity, this value of ω does not satisfy Eq. (12) for any integer l ($\mu \approx 0.59E_F$ and $\Delta_0 \approx 0.69E_F$ at $1/k_F a = 0$ in the mean-field theory), so there is only one peak and dip for each value of l: there are two peaks in n_k and F_k at $k/k_F \approx 1.4$ and 1.9, which correspond to the fundamental harmonic ($l = 1$) and the second harmonic ($l = 2$), respectively. Figures 4(e) and 4(f) show the case for $1/k_F a = 1$ as an example on the BEC side. Since $\mu < 0$ at $1/k_F a = 1$, the quasiparticle spectrum E_k is monotonically increasing with k, so the resonance condition (11) for each value of l can yield only a single peak and dip. As a representative example, we set $\omega = 3E_F/\hbar$ smaller than the threshold frequency $\omega_{\rm th} \lesssim 2\sqrt{\mu^2 + \Delta^2} \approx 3.11E_F/\hbar$ for $\mu \approx -0.80E_F$ and $\Delta_0 \approx 1.33E_F$ at $1/k_F a = 1$. Note that, even though $\omega < \omega_{\rm th}$, there is a resonance peak around $k/k_F \approx 1.24$ which is given by the second harmonic $l = 2$.

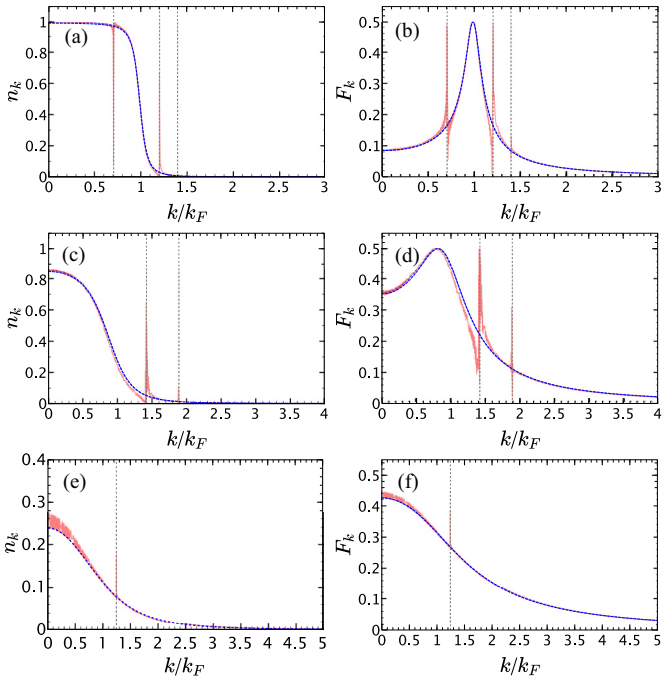

FIG. 4. Resonance peaks in n_k and F_k for $1/k_F a = -1$ [(a) and (b)], $1/k_F a = 0$ [(c) and (d)], and $1/k_F a = 1$ [(e) and (f)]. The red solid line shows the snapshot at $t = 2000/(E_F/\hbar)$, and the blue dashed line shows the initial equilibrium state. Here, the modulation amplitude $A = 0.01$. For (a) and (b), the modulation frequency is $\omega = 1E_F/\hbar$, and the vertical dotted lines are obtained from the conditions $2E_k = \hbar\omega$, $\hbar\omega$, and $2\hbar\omega$, respectively (from left to right). For (c) and (d), the modulation frequency is $\omega = 3E_F/\hbar$, and the vertical dotted line is obtained from the conditions $2E_k = \hbar\omega$ and $2\hbar\omega$, respectively (from left to right). For (e) and (f), the modulation frequency is $\omega = 3E_F/\hbar$, and the vertical dotted line is obtained from the condition $2E_k = 2\hbar\omega$.

For larger modulation amplitudes A, resonance peaks and dips grow much faster. Figure 5 shows the result for $A = 0.3$ at $t = 2000/(E_F/\hbar)$, where many resonance peaks in n_k

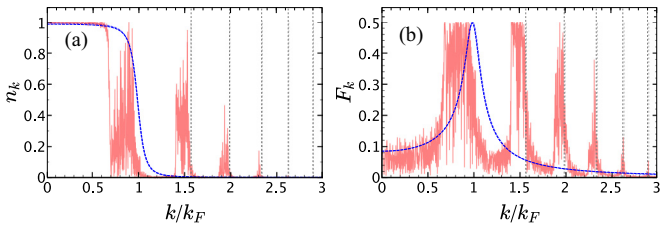

FIG. 5. Resonance peaks in (a) n_k and (b) F_k for large-amplitude modulation with $A = 0.3$ for $1/k_F a = -1$ and $\omega = 3E_F/\hbar$. The red solid line shows the snapshot at $t = 2000/(E_F/\hbar)$, and the blue dashed line shows the initial equilibrium state. The vertical dotted lines correspond to $2E_k = \hbar\omega$, $2\hbar\omega$, $3\hbar\omega$, $4\hbar\omega$, and $5\hbar\omega$, respectively (from left to right), in both panels.

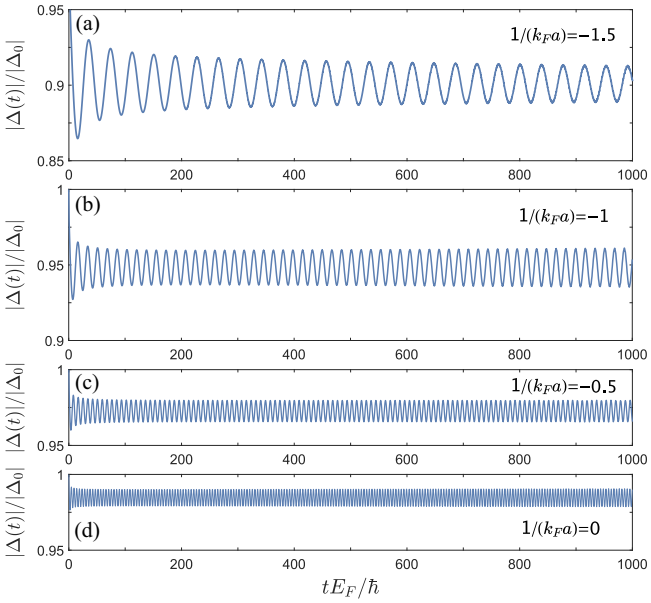

FIG. 6. Long-lived Higgs-mode oscillations excited by removing particles in superfluid Fermi gases with different $1/k_F a$. Five percent of the particles are removed around the wave number $k_{\rm hole}$ at $k_{\rm hole}/k_F = 0.989, 0.975, 0.93$, and 0.79 in (a)–(d), respectively. Here, we take $E_c = 100E_F$.

and F_k caused by the higher harmonics can clearly be seen. In this example, we set $\omega = 3E_F/\hbar$, so that the first resonance peak of $l = 1$ is located far above the Fermi wave number, $k \approx 1.57k_F$. Since many particles are excited to the resonance peaks above the Fermi energy, the distribution n_k of the particles below the Fermi energy is largely depleted from the initial equilibrium state shown by the blue dashed line.

IV. LONG-LIVED HIGGS MODE EXCITED BY PARTICLE REMOVAL

In this section, we propose an alternative scheme to excite long-lived Higgs-mode oscillations. This scheme consists of removing particles around a certain magnitude of the momentum (denoted by $\hbar k_{\rm hole}$), which can be realized by, e.g., shining red-detuned lasers, which will be discussed in detail in the next section. Removing particles can be regarded as an alternative to the conventional way of quenching through parameter change. As we shall demonstrate below, an advantage of this scheme is that very long-lived Higgs-mode oscillations with relatively large amplitude can be produced in a wide region in the crossover from the BCS limit ($1/k_F a \ll -1$) to the unitary regime ($1/k_F \approx 0$).

Figure 6 shows the resulting long-lived Higgs-mode oscillations excited using this scheme for several values of $1/k_F a$. In the simulation, we first prepare the equilibrium state for a given value of $1/k_F a$ and then remove the particles around the wave number $k_{\rm hole}$. For the cases in Figs. 6(a)–6(d), we set $k_{\rm hole}/k_F = 0.989,\ 0.975,\ 0.93$, and 0.79, respectively, and the number of removed particles δnV is 5% of the total number of particles (i.e., $\delta n/n = 5\%$). Specifically, in the simulations, we remove the particles in a finite range of k around $k_{\rm hole}$ with the width $2\delta k$, i.e., $k_{\rm hole} - \delta k \leqslant k \leqslant k_{\rm hole} + \delta k$. The width $2\delta k$ is determined by the number of removed particles based on the following condition:

$$\delta n = 2 \int_{|k-k_{\rm hole}|\leqslant \delta k} n_k \, d^3k \tag{13}$$

with n_k for the initial equilibrium state. The oscillation frequency of $|\Delta(t)|$ in each panel is around $2\Delta_0/\hbar$, which agrees with the Higgs-mode frequency. It is noted that, after the oscillation amplitude stabilizes, $|\Delta(t)|$ does not show a decaying oscillation [see, e.g., Figs. 6(b)–6(d)]. Rather, the amplitude even gradually increases after the stabilization: in a very long timescale, the amplitude of the oscillation gradually increases to a maximum value and then decreases to a nonzero minimum value repeatedly. The time t_1 corresponding to the first maximum amplitude, which characterizes the duration of the constant amplitude, serves as a reasonable measure for the effective lifetime of the Higgs mode in the present case.

We study the Higgs mode excitation by removing particles at various values of $k_{\rm hole}$ for different $1/k_F a$. The results are summarized in Fig. 7: Figs. 7(a) and 7(b) show the case of $\delta n/n = 5\%$, and Figs. 7(c) and 7(d) show $\delta n/n = 10\%$. Figure 7(a) shows the time t_1 as a function of $k_{\rm hole}$. We observe that the long-lived Higgs mode is excited only in a certain range of $k_{\rm hole}$, and the range of $k_{\rm hole}$ changes with $1/k_F a$. In the unitary regime ($1/k_F a \approx 0$), the range of $k_{\rm hole}$ to excite the long-lived Higgs mode is wider than that in the BCS regime ($1/k_F a < 0$). The long-lived Higgs-mode oscillations shown in Fig. 6 are realized for a particular value of $k_{\rm hole}$ corresponding to the resonance peak in Fig. 7(a).

Figure 7(b) shows the maximum amplitude at t_1 relative to Δ_0 as a function of $k_{\rm hole}$. The maximum relative amplitude becomes larger by going towards the deeper BCS regime. On the other hand, it is hard to excite a Higgs-mode oscillation with a larger amplitude in the BEC regime ($1/k_F a > 0$, not shown) using the present scheme. Note that the relative amplitude shows a dip at the wave number $k_{\rm hole}$, corresponding to the resonance peak location in Fig. 7(a). This dip can be understood as follows. When we have a long-lived Higgs-mode oscillation with $t_1 = \infty$ at $k_{\rm hole}$ corresponding to the resonance peak location, no other modes except for the Higgs mode are excited. However, if $k_{\rm hole}$ slightly deviates from the resonance, not only the Higgs mode but other modes are also excited, so that the oscillation resulting from the superposition of these different excited modes has a larger amplitude compared to the former case of only the Higgs-mode excitation.

Next, we compare the cases with different fractions of removed particles. Figures 7(c) and 7(d) are the same as Figs. 7(a) and 7(b), respectively, except for $\delta n/n = 10\%$. In comparison of Figs. 7(a) and 7(b) for $\delta n/n = 5\%$ and Figs. 7(c) and 7(d) for $\delta n/n = 10\%$, the effective lifetime t_1 is almost the same in the two cases, but the amplitude of the oscillation for $\delta n/n = 10\%$ is roughly double that for $\delta n/n = 5\%$ [see Figs. 7(b) and 7(d)]. This means that the amplitude of the excited Higgs-mode oscillation can be controlled by tuning the number of removed particles $\delta n/n$ in the present scheme. It should also be noted that, even in the case of $\delta n/n = 5\%$, the relative amplitude, which is of the order

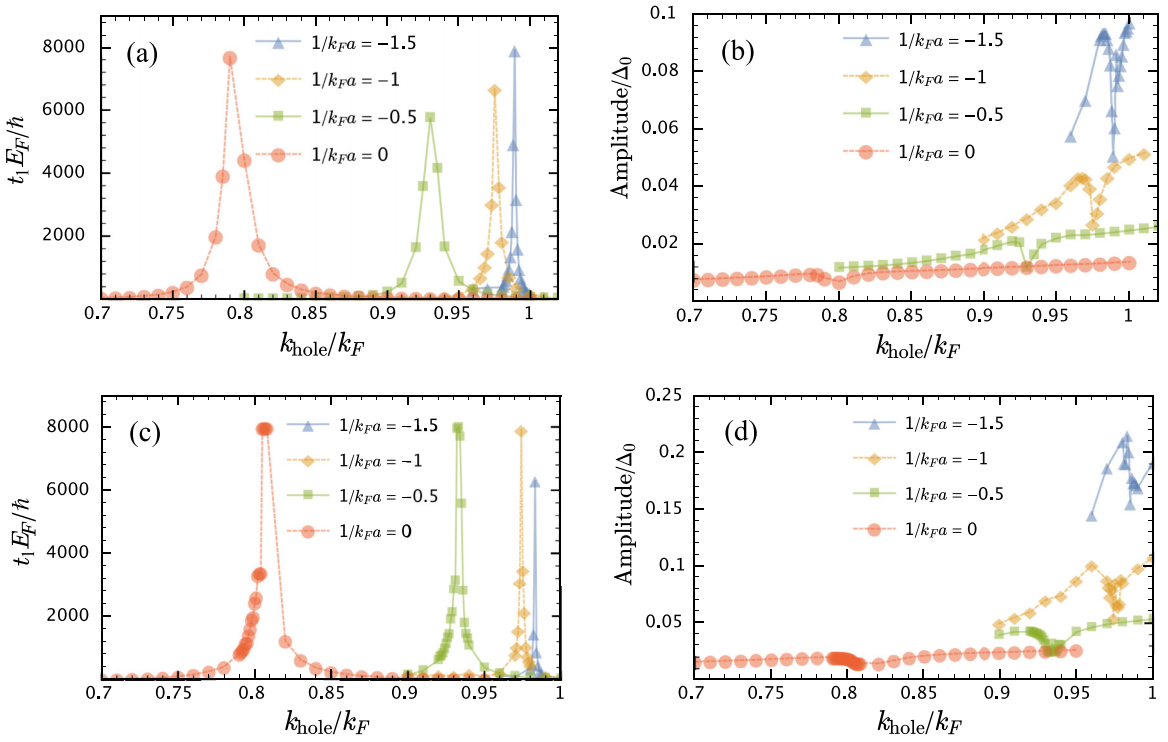

FIG. 7. Time t_1 at which the oscillation amplitude takes the maximum value for the first time [(a) and (b)] and the relative amplitude at t_1 [(b) and (d)] as a function of $k_{\rm hole}$ for different values of $1/k_Fa$. The number of removed particles is $\delta n/n = 5\%$ in (a) and (b) and 10% in (c) and (d). The cutoff energy E_c is taken at $100E_F$ for all the cases in (a) and (b). In (c) and (d), we take $E_c = 16E_F$ for $1/k_Fa = -1.5$ and -1 and $E_c = 36E_F$ for $1/k_Fa = -0.5$ and 0.

of 1% [see Fig. 7(b)], is much larger than that in a recent experiment [17], which was only of the order of 0.1%.

Finally, we remark that the wave number $k_{\rm hole}$ of the resonance peak in Figs. 7(a) and 7(c) coincides with the wave number $k_{\rm peak}$ at the peak location of the pair wave function F_k in the equilibrium state [see, e.g., the blue dashed lines in Figs. 4(b) and 4(d)]. Thus, one can deduce from the pair wave function F_k the appropriate value of $k_{\rm hole}$ for exciting the Higgs mode. Since the peak of F_k at nonzero k disappears in the BEC regime of $1/k_Fa \gtrsim 0.5$, our scheme is applicable for exciting the long-lived Higgs-mode oscillation up to the shallow BEC side of $1/k_Fa \lesssim 0.5$.

V. SUMMARY AND CONCLUDING REMARKS

Finally, we shall provide two possible methods for experimental realization of particle removal. The first method is to use resonant laser beams to transfer atoms with certain momenta to an untrapped internal state. Taking a quasi-one-dimensional Fermi gas, e.g., an elongated Fermi gas along the x direction in a tight trap in the y and z directions, we shine two counterpropagating red-detuned lasers with wave number q and detuning δ in the $\pm x$ directions to resonantly excite the atoms around certain momenta $\pm\hbar k_x = \pm m\delta/q$. Here, the excited state is supposed to be an untrapped state of the external potential. Note that the untrapped excited state should have a narrow natural linewidth to make the momentum selection accurate enough compared to the width $\Delta k_{\rm hole}$ of the peaks in Figs. 7(a) and 7(c) [typically, $\Delta k_{\rm hole} = O(10^{-2})\,k_F$]. The clock states [usually with a natural linewidth on the order of $O(10)$ mHz] can fulfill this requirement very well. For example, there is a clock state with a linewidth of 38.5 mHz for ^{173}Yb [67]. A degenerate Fermi gas of ^{173}Yb realized in Ref. [68] has a Fermi temperature $T_F \approx 2 \times 10^2$ nK, corresponding to the Fermi energy $E_F/h \approx 4$ kHz. Therefore, the linewidth of the clock state is negligible compared to the energy width $\Delta E_{\rm hole}$ corresponding to the region within $\Delta k_{\rm hole}$ around $k_{\rm hole}$: $\Delta E_{\rm hole} \sim \hbar^2(k_{\rm hole} + \Delta k_{\rm hole})^2/2m - \hbar^2 k_{\rm hole}^2/2m \simeq 2\hbar^2 k_{\rm hole}\,\Delta k_{\rm hole}/2m \sim O(10^2)$ Hz $\times h$ for $k_{\rm hole} \sim k_F$ and $\Delta k_{\rm hole} = O(10^{-2})\,k_F$. Thus, the momentum can be selected accurately provided the laser frequency is well locked.

The second method is to make the g modulation (see Sec. III B) with frequency $\omega \simeq 2\Delta_0/\hbar$ to make a resonance at the wave number $k_{\rm peak}$ corresponding to the peak of the pair wave function F_k. Here, we keep this g modulation for a while to generate a deep dip at $k_{\rm peak}$ and then turn off the modulation. The resulting F_k with a deep dip at $k_{\rm peak}$ can be used as an initial state for the time evolution. To avoid other excitations, we need to tune the amplitude and the duration of the g modulation and reduce the amplitude slowly. In practice, the duration of the modulation should be long enough to make a deep dip at $k_{\rm peak}$, and the amplitude of the modulation has to be small enough to avoid exciting other modes. We find that this method can also generate Higgs-mode oscillations with a relatively long lifetime. However, because we cannot completely avoid other excitations, the oscillation decays in time, unlike in the first scheme of removing particles directly. Figure 8 shows an example of the result from this method. There, we

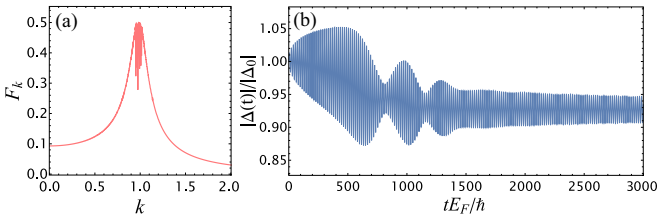

FIG. 8. A Higgs-mode oscillation caused by removing particles using g modulation. Here, we take $1/k_F a = -1$ and modulation frequency $\omega = 1.97\,|\Delta_0|/\hbar$. The modulation amplitude is constant at $A = 0.001$ from $t = 0$ to $1000\,\hbar/E_F$ and is then reduced to zero linearly from $t = 1000\,\hbar/E_F$ to $1500\,\hbar/E_F$. (a) shows F_k at $t = 1500\,\hbar/E_F$ with a dip around k_{peak}. (b) shows the oscillation of the magnitude of the order parameter $\Delta(t)$ during the whole process. Here, we take $E_c = 100\,E_F$.

perform g modulation with a constant amplitude from $t = 0$ to $1000\,\hbar/E_F$ and then reduce the modulation amplitude to zero linearly from $t = 1000\,\hbar/E_F$ to $1500\,\hbar/E_F$. Then, the system undergoes free evolution from $t = 1500\hbar/E_F$. At $t = 1500\,\hbar/E_F$ just after removing the modulation, F_k has a relatively deep dip around k_{peak} [Fig. 8(a)], and then $|\Delta(t)|$ shows a quite stable oscillation from $t = 1500\,\hbar/E_F$ [Fig. 8(b)]. However, it is clearly discernible from Fig. 8(b) that the amplitude of the oscillation decreases, albeit slowly, in time (until it becomes irregular after very long time, which is not shown), unlike the results from direct removal of particles [see, e.g., Figs. 6(b)–6(d)].

In summary, we have proposed a scheme to generate long-lived Higgs-mode oscillations in a homogeneous superfluid Fermi gas at zero temperature. First, we discussed the excitation of the Higgs mode by time-periodic modulation of the scattering length. Although Higgs-mode oscillations can be produced by this method, higher-harmonic excitations are also inevitably generated by the "parametric up-conversion" due to nonlinearity in the superfluid phase. Then, we proposed an alternative scheme to excite the Higgs mode by removing particles around a certain absolute value of momentum $\hbar k_{\text{hole}}$. The removal of particles can also be regarded as an unconventional type of quench. This scheme can generate very stable Higgs-mode oscillations with much longer lifetime and larger amplitude compared with a recent experiment [17]. We have demonstrated that persistent Higgs-mode oscillations with almost constant amplitude can be produced (see Fig. 6). These persistent oscillations can be realized by tuning k_{hole} to k_{peak}, where k_{peak} is the wave number corresponding to the peak of the pair wave function F_k in equilibrium. Furthermore, the amplitude of the Higgs-mode oscillation can be controlled by the number of removed particles. Finally, we proposed two ways to realize particle removal in experiment. It should be mentioned that our discussions are based on the uniform system. Nevertheless, given that preparing a quasihomogeneous system using a box potential is a fairly mature experimental technique [69], our scheme can be readily implemented experimentally. We leave the case of a harmonic trapping potential to future work.

ACKNOWLEDGMENTS

We thank B. P. Venkatesh for helpful discussions and comments. G.W. was supported by the NSF of China (Grants No. 11975199 and No. 11674283), by the Zhejiang Provincial Natural Science Foundation Key Project (Grant No. LZ19A050001), and by the Zhejiang University 100 Plan. Q.C. was supported by the NSF of China (Grant No. 11774309) and the Innovation Program for Quantum Science and Technology (Grant No. 2021ZD0301904). K.-T.X. was supported by the MOST of China (Grant No. G2022181023L) and NUAA (Grant No. YAT22005). G.L. and K.-T.X. contributed equally to this work.

[1] F. Englert and R. Brout, Broken Symmetry and the Mass of Gauge Vector Mesons, Phys. Rev. Lett. **13**, 321 (1964).

[2] P. W. Higgs, Broken Symmetries and the Masses of Gauge Bosons, Phys. Rev. Lett. **13**, 508 (1964).

[3] G. S. Guralnik, C. R. Hagen, and T. W. B. Kibble, Global Conservation Laws and Massless Particles, Phys. Rev. Lett. **13**, 585 (1964).

[4] D. Pekker and C. M. Varma, Amplitude/Higgs modes in condensed matter physics, Annu. Rev. Condens. Matter Phys. **6**, 269 (2015).

[5] R. Shimano and N. Tsuji, Higgs mode in superconductors, Annu. Rev. Condens. Matter Phys. **11**, 103 (2020).

[6] G. E. Volovik and M. A. Zubkov, Higgs bosons in particle physics and in condensed matter, J. Low Temp. Phys. **175**, 486 (2014).

[7] R. Sooryakumar and M. V. Klein, Raman Scattering by Superconducting-Gap Excitations and Their Coupling to Charge-Density Waves, Phys. Rev. Lett. **45**, 660 (1980).

[8] U. Bissbort, S. Götze, Y. Li, J. Heinze, J. S. Krauser, M. Weinberg, C. Becker, K. Sengstock, and W. Hofstetter, Detecting the Amplitude Mode of Strongly Interacting Lattice Bosons by Bragg Scattering, Phys. Rev. Lett. **106**, 205303 (2011).

[9] M. Endres, T. Fukuhara, D. Pekker, M. Cheneau, P. Schauß, C. Gross, E. Demler, S. Kuhr, and I. Bloch, The 'Higgs' amplitude mode at the two-dimensional superfluid/Mott insulator transition, Nature (London) **487**, 454 (2012).

[10] R. Matsunaga, Y. I. Hamada, K. Makise, Y. Uzawa, H. Terai, Z. Wang, and R. Shimano, Higgs Amplitude Mode in the BCS Superconductors $Nb_{1-x}Ti_xN$ Induced by Terahertz Pulse Excitation, Phys. Rev. Lett. **111**, 057002 (2013).

[11] B. Mansart, J. Lorenzana, A. Mann, A. Odeh, M. Scarongella, M. Chergui, and F. Carbone, Coupling of a high-energy excitation to superconducting quasiparticles in a cuprate from coherent charge fluctuation spectroscopy, Proc. Natl. Acad. Sci. USA **110**, 4539 (2013).

[12] D. Sherman, U. S. Pracht, B. Gorshunov, S. Poran, J. Jesudasan, M. Chand, P. Raychaudhuri, M. Swanson, N. Trivedi, A. Auerbach, M. Scheffler, A. Frydman, and M. Dressel, The Higgs mode in disordered superconductors close to a quantum phase transition, Nat. Phys. **11**, 188 (2015).

[13] T. M. Hoang, H. M. Bharath, M. J. Boguslawski, M. Anquez, B. A. Robbins, and M. S. Chapman, Adiabatic quenches and characterization of amplitude excitations in a continuous quantum phase transition, Proc. Natl. Acad. Sci. USA **113**, 9475 (2016).

[14] A. Jain, M. Krautloher, J. Porras, G. H. Ryu, D. P. Chen, D. L. Abernathy, J. T. Park, A. Ivanov, J. Chaloupka, G. Khaliullin, B. Keimer, and B. J. Kim, Higgs mode and its decay in a two-dimensional antiferromagnet, Nat. Phys. **13**, 633 (2017).

[15] T. Hong, M. Matsumoto, Y. Qiu, W. Chen, T. R. Gentile, S. Watson, F. F. Awwadi, M. M. Turnbull, S. E. Dissanayake, H. Agrawal, R. Toft-Petersen, B. Klemke, K. Coester, K. P. Schmidt, and D. A. Tennant, Higgs amplitude mode in a two-dimensional quantum antiferromagnet near the quantum critical point, Nat. Phys. **13**, 638 (2017).

[16] J. Léonard, A. Morales, P. Zupancic, T. Donner, and T. Esslinger, Monitoring and manipulating Higgs and Goldstone modes in a supersolid quantum gas, Science **358**, 1415 (2017).

[17] A. Behrle, T. Harrison, J. Kombe, K. Gao, M. Link, J.-S. Bernier, C. Kollath, and M. Köhl, Higgs mode in a strongly interacting fermionic superfluid, Nat. Phys. **14**, 781 (2018).

[18] ATLAS Collaboration, Observation of a new particle in the search for the standard model Higgs boson with the ATLAS detector at the LHC, Phys. Lett. B **716**, 1 (2012).

[19] CMS Collaboration, Observation of a new boson at a mass of 125 GeV with the CMS experiment at the LHC, Phys. Lett. B **716**, 30 (2012).

[20] A. F. Volkov and Sh. M. Kogan, Collisionless relaxation of the energy gap in superconductors, Zh. Eksp. Teor. Fiz. **65**, 2038 (1973) [Sov. Phys. JETP **38**, 1018 (1974)].

[21] V. Gurarie, Nonequilibrium Dynamics of Weakly and Strongly Paired Superconductors, Phys. Rev. Lett. **103**, 075301 (2009).

[22] P. B. Littlewood and C. M. Varma, Gauge-Invariant Theory of the Dynamical Interaction of Charge Density Waves and Superconductivity, Phys. Rev. Lett. **47**, 811 (1981).

[23] P. B. Littlewood and C. M. Varma, Amplitude collective modes in superconductors and their coupling to charge-density waves, Phys. Rev. B **26**, 4883 (1982).

[24] B. DeMarco and D. S. Jin, Onset of Fermi degeneracy in a trapped atomic gas, Science **285**, 1703 (1999).

[25] A. V. Andreev, V. Gurarie, and L. Radzihovsky, Nonequilibrium Dynamics and Thermodynamics of a Degenerate Fermi Gas across a Feshbach Resonance, Phys. Rev. Lett. **93**, 130402 (2004).

[26] R. A. Barankov, L. S. Levitov, and B. Z. Spivak, Collective Rabi Oscillations and Solitons in a Time-Dependent BCS Pairing Problem, Phys. Rev. Lett. **93**, 160401 (2004).

[27] M. H. Szymańska, B. D. Simons, and K. Burnett, Dynamics of the BCS-BEC Crossover in a Degenerate Fermi Gas, Phys. Rev. Lett. **94**, 170402 (2005).

[28] E. A. Yuzbashyan, O. Tsyplyatyev, and B. L. Altshuler, Relaxation and Persistent Oscillations of the Order Parameter in Fermionic Condensates, Phys. Rev. Lett. **96**, 097005 (2006).

[29] R. A. Barankov and L. S. Levitov, Synchronization in the BCS Pairing Dynamics as a Critical Phenomenon, Phys. Rev. Lett. **96**, 230403 (2006).

[30] A. Bulgac and S. Yoon, Large Amplitude Dynamics of the Pairing Correlations in a Unitary Fermi Gas, Phys. Rev. Lett. **102**, 085302 (2009).

[31] S. Hannibal, P. Kettmann, M. D. Croitoru, A. Vagov, V. M. Axt, and T. Kuhn, Quench dynamics of an ultracold Fermi gas in the BCS regime: Spectral properties and confinement-induced breakdown of the Higgs mode, Phys. Rev. A **91**, 043630 (2015).

[32] S. Yoon and G. Watanabe, Pairing Dynamics of Polar States in a Quenched p-Wave Superfluid Fermi Gas, Phys. Rev. Lett. **119**, 100401 (2017).

[33] S. Hannibal, P. Kettmann, M. D. Croitoru, V. M. Axt, and T. Kuhn, Persistent oscillations of the order parameter and interaction quench phase diagram for a confined Bardeen-Cooper-Schrieffer Fermi gas, Phys. Rev. A **98**, 053605 (2018).

[34] G. Seibold and J. Lorenzana, Nonequilibrium dynamics from BCS to the bosonic limit, Phys. Rev. B **102**, 144502 (2020).

[35] H. P. Collado, N. Defenu, and J. Lorenzana, Engineering Higgs dynamics by spectral singularities, arXiv:2205.06826.

[36] W. Yi and L.-M. Duan, Dynamic response of an ultracold Fermi gas near the Feshbach resonance, Phys. Rev. A **73**, 013609 (2006).

[37] R. G. Scott, F. Dalfovo, L. P. Pitaevskii, and S. Stringari, Rapid ramps across the BEC-BCS crossover: A route to measuring the superfluid gap, Phys. Rev. A **86**, 053604 (2012).

[38] J. Tokimoto, S. Tsuchiya, and T. Nikuni, Excitation of Higgs mode in superfluid Fermi gas in BCS-BEC crossover, J. Phys. Soc. Jpn. **88**, 023601 (2019).

[39] H. P. Ojeda Collado, J. Lorenzana, G. Usaj, and C. A. Balseiro, Population inversion and dynamical phase transitions in a driven superconductor, Phys. Rev. B **98**, 214519 (2018).

[40] H. P. Ojeda Collado, G. Usaj, J. Lorenzana, and C. A. Balseiro, Nonlinear dynamics of driven superconductors with dissipation, Phys. Rev. B **101**, 054502 (2020).

[41] H. P. Ojeda Collado, G. Usaj, C. A. Balseiro, D. H. Zanette, and J. Lorenzana, Emergent parametric resonances and time-crystal phases in driven Bardeen-Cooper-Schrieffer systems, Phys. Rev. Res. **3**, L042023 (2021).

[42] G. M. Bruun, Low-Energy Monopole Modes of a Trapped Atomic Fermi Gas, Phys. Rev. Lett. **89**, 263002 (2002).

[43] A. Korolyuk, J. J. Kinnunen, and P. Törmä, Density response of a trapped Fermi gas: A crossover from the pair vibration mode to the Goldstone mode, Phys. Rev. A **84**, 033623 (2011).

[44] D. Podolsky, A. Auerbach, and D. P. Arovas, Visibility of the amplitude (Higgs) mode in condensed matter, Phys. Rev. B **84**, 174522 (2011).

[45] B. Liu, H. Zhai, and S. Zhang, Evolution of the Higgs mode in a fermion superfluid with tunable interactions, Phys. Rev. A **93**, 033641 (2016).

[46] X. Han, B. Liu, and J. Hu, Observability of Higgs mode in a system without Lorentz invariance, Phys. Rev. A **94**, 033608 (2016).

[47] C. M. Varma, Higgs boson in superconductors, J. Low Temp. Phys. **126**, 901 (2002).

[48] A. Akbari, A. P. Schnyder, D. Manske, and I. Eremin, Theory of nonequilibrium dynamics of multiband superconductors, Europhys. Lett. **101**, 17002 (2013).

[49] S. Maiti and P. J. Hirschfeld, Collective modes in superconductors with competing s- and d-wave interactions, Phys. Rev. B **92**, 094506 (2015).

[50] M. A. Müller, P. Shen, M. Dzero, and I. Eremin, Short-time dynamics in $s + is$-wave superconductor with incipient bands, Phys. Rev. B **98**, 024522 (2018).

[51] D. Fausti, R. Tobey, N. Dean, S. Kaiser, A. Dienst, M. C. Hoffmann, S. Pyon, T. Takayama, H. Takagi, and A. Cavalleri, Light-induced superconductivity in a stripe-ordered cuprate, Science **331**, 189 (2011).

[52] S. Kaiser, C. R. Hunt, D. Nicoletti, W. Hu, I. Gierz, H. Y. Liu, M. Le Tacon, T. Loew, D. Haug, B. Keimer, and A. Cavalleri, Optically induced coherent transport far above T_c in underdoped $YBa_2Cu_3O_{6+\delta}$, Phys. Rev. B **89**, 184516 (2014).

[53] W. Hu, S. Kaiser, D. Nicoletti, C. R. Hunt, I. Gierz, M. C. Hoffmann, M. Le Tacon, T. Loew, B. Keimer, and A. Cavalleri, Optically enhanced coherent transport in $YBa_2Cu_3O_{6.5}$ by ultrafast redistribution of interlayer coupling, Nat. Mater. **13**, 705 (2014).

[54] M. Mitrano, A. Cantaluppi, D. Nicoletti, S. Kaiser, A. Perucchi, S. Lupi, P. Di Pietro, D. Pontiroli, M. Riccò, S. R. Clark, D. Jaksch, and A. Cavalleri, Possible light-induced superconductivity in K_3C_{60} at high temperature, Nature (London) **530**, 461 (2016).

[55] G. M. Bruun, Long-lived Higgs mode in a two-dimensional confined Fermi system, Phys. Rev. A **90**, 023621 (2014).

[56] P. G. de Gennes, *Superconductivity of Metals and Alloys* (CRC Press, Boca Raton, FL, 1966).

[57] R. Kümmel, Dynamics of current flow through the phase-boundary between a normal and a superconducting region, Z. Phys. A **218**, 472 (1969).

[58] J. B. Ketterson and S. N. Song, *Superconductivity* (Cambridge University Press, Cambridge, 1999).

[59] A. J. Leggett, Diatomic molecules and Cooper pairs, in *Modern Trends in the Theory of Condensed Matter*, edited by A. Pękalski and J. A. Przystawa (Springer, Berlin, 1980), pp. 13–27.

[60] M. Randeria, Crossover from BCS theory to Bose-Einstein condensation, in *Bose-Einstein Condensation*, edited by A. Griffin, D. W. Snoke, and S. Stringari (Cambridge University Press, Cambridge, 1995), pp. 355–392.

[61] S. Giorgini, L. P. Pitaevskii, and S. Stringari, Theory of ultracold atomic Fermi gases, Rev. Mod. Phys. **80**, 1215 (2008).

[62] M. Greiner, C. A. Regal, and D. S. Jin, Probing the Excitation Spectrum of a Fermi Gas in the BCS-BEC Crossover Regime, Phys. Rev. Lett. **94**, 070403 (2005).

[63] S. T. Thompson, E. Hodby, and C. E. Wieman, Ultracold Molecule Production via a Resonant Oscillating Magnetic Field, Phys. Rev. Lett. **95**, 190404 (2005).

[64] L. W. Clark, A. Gaj, L. Feng, and C. Chin, Collective emission of matter-wave jets from driven Bose–Einstein condensates, Nature (London) **551**, 356 (2017).

[65] C. Chin, R. Grimm, P. Julienne, and E. Tiesinga, Feshbach resonances in ultracold gases, Rev. Mod. Phys. **82**, 1225 (2010).

[66] A. Yariv, *Quantum Electronics*, 3rd ed. (Wiley, New York, 1988).

[67] S. G. Porsev and A. Derevianko, Hyperfine quenching of the metastable $^3P_{0,2}$ states in divalent atoms, Phys. Rev. A **69**, 042506 (2004).

[68] T. Fukuhara, Y. Takasu, M. Kumakura, and Y. Takahashi, Degenerate Fermi Gases of Ytterbium, Phys. Rev. Lett. **98**, 030401 (2007).

[69] A. L. Gaunt, T. F. Schmidutz, I. Gotlibovych, R. P. Smith, and Z. Hadzibabic, Bose-Einstein Condensation of Atoms in a Uniform Potential, Phys. Rev. Lett. **110**, 200406 (2013).